

Do the observational data favor a local void?Rong-Gen Cai,^{1,2,3,*} Jia-Feng Ding,^{1,2,†} Zong-Kuan Guo,^{1,2,3,‡} Shao-Jiang Wang,^{2,4,§} and Wang-Wei Yu^{1,2,||}¹*School of Physical Sciences, University of Chinese Academy of Sciences (UCAS), Beijing 100049, China*²*CAS Key Laboratory of Theoretical Physics, Institute of Theoretical Physics, Chinese Academy of Sciences, P.O. Box 2735, Beijing 100190, China*³*School of Fundamental Physics and Mathematical Sciences, Hangzhou Institute for Advanced Study (HIAS), University of Chinese Academy of Sciences, Hangzhou 310024, China*⁴*Quantum Universe Center and School of Physics, Korea Institute for Advanced Study (KIAS), Seoul 02455, Korea* (Received 22 December 2020; revised 17 April 2021; accepted 24 May 2021; published 22 June 2021)

The increasing tension between the different local direct measurements of the Hubble expansion rate and that inferred from the cosmic microwave background observation by the Λ -cold-dark-matter model could be a smoking gun of new physics, if not caused by either observational systematics or local bias. We generalize previous investigation on the local bias from a local void by globally fitting the Pantheon sample over all parameters in the radial profile function of a local void described by an inhomogeneous but isotropic Lemaître-Tolman-Bondi metric with a cosmological constant. Our conclusion strengthens the previous studies that the current tension on Hubble constant cannot be saved by a local void alone.

DOI: [10.1103/PhysRevD.103.123539](https://doi.org/10.1103/PhysRevD.103.123539)**I. INTRODUCTION**

The precision cosmology from the local observations of the type Ia supernovae (SNe Ia) [1,2] and the global observations of the cosmic microwave background (CMB) [3–5] has favored the dubbed Λ -cold-dark-matter (Λ CDM) model [6–8] as the concordance model withstanding many other data testings in the last two decades but with a notable exception for the increasing tension on the Hubble constant (2.5σ [9], 3.4σ [10], 3.7σ [11], 3.8σ [12], 4.4σ [13], 4.7σ [14], and 5.3σ [15]) between the local and global observations [16], which, if not caused by either systematics errors or local bias, could be the smoking gun of new physics [17] beyond the Λ CDM model either from the early or late Universe [16,18,19]. Therefore, it is crucial to rule out the resolution from the possibility of, for example, a local void [20–24].

A cosmic void with its matter distribution changing in the radial coordinate could be described by the dubbed Lemaître-Tolman-Bondi (LTB) [25–27] metric for an inhomogeneous but isotropic Universe we might live in locally [28–32]. However, some constraints from the detection of the secondary CMB effect like kinetic Sunyaev-Zel’dovich (kSZ) effect [33,34] have ruled out a class of giant local dust void models [35] (see, however,

[36] for a recent attempt to ease the Hubble tension but still evading the kSZ limit). Nevertheless, the LTB model with a cosmological constant, called the Λ LTB model, still seems to be able to relieve [37–39] or even fully resolve [40–42] the Hubble tension when using the galaxy survey data. For example, the luminosity density sample [43–46] is constructed over the redshift range $0.01 < z < 0.2$ for the discovery of the Keenan-Barger-Cowie (KBC) void [21] with a size of ~ 300 Mpc and density contrast of -30% . In particular, by adopting a radial profile for the matter density fraction with the Garcia-Ballido-Haugbølle (GBH) parameterization [47] smoothly connecting two homogeneous parts inside and outside a local underdensity, Hoscheit and Barger [41] have fitted the SNe Ia data in the redshift range $0.0233 < z < 0.15$ and then reduced the Hubble tension from 3.4σ to 2.75σ with the GBH parameters fixed by the KBC void configuration.

However, the data analysis of [41] was revised by Kenworthy, Scolnic, and Riess in [48] by using a larger sample of low-redshift SNe from a combined sample of the Pantheon, Foundation, and Carnegie-Supernova-Project (CSP) samples within $z < 0.5$ with fully appreciating for systematic uncertainties in the SNe data, such as uncertainties in the nuisance parameters, calibration uncertainties, and possible redshift evolution of the nuisance parameters. Furthermore, Kenworthy, Scolnic, and Riess [48] also adopted more physically motivated boundary conditions, such as the GBH parameterization for the physical matter density profile $\rho_M(r)$ instead of the dimensionless matter density fraction $\Omega_M(r)$ used in [41],

*cairg@itp.ac.cn

†dingjiafeng@itp.ac.cn

‡guozk@itp.ac.cn

§schwang@cosmos.phy.tufts.edu

||yuwangwei@mail.itp.ac.cn

and the treatment of the time since the big bang t_B as a free constant parameter instead of the inappropriate choice $t_B(r) = r$ used in [41]. Nevertheless, the GBH profile in [48] was also fixed by the same KBC void configuration. The conclusion drawn from [48] agrees well with previous studies [38,49,50] that the cosmic void for the Hubble constant determination fitted by the Hubble diagram is inadequate to account for the current discrepancy of the Hubble tension. Later in [51] the GBH parameterization was chosen for the spatial curvature in order to achieve a complete analytic determination of the cosmic time in terms of the radial coordinate suitable for fitting the void size from a top-hat profile. Consistent with Kenworthy, Scolnic, and Riess in [48], the local void fitted by the low-redshift Pantheon SNe data in [51] is also insufficient to resolve the Hubble tension, in contrast to the luminosity distance data that admit a large local void.

Although [48] has ruled out a local void with a sharp edge and depth $|\Delta\delta| > 20\%$ in the redshift range $0.023 < z < 0.15$ by fitting the GBH matter profile to the combined SNe data sample (Pantheon, Foundation and CSP) within $z < 0.5$, this does not automatically rule out a larger void with a shallower depth and a wider edge in a larger sample of SNe data. The void search from [51] has used the full data of Pantheon sample but the GBH profile has been imposed on the spatial curvature term instead of the matter density fraction. Besides, a mild tension ($2 - 3\sigma$) was found in [52] in the context of the Λ CDM model (instead of the Λ LTB model) between the best fit value of $\mathcal{M} \equiv M + 5 \log_{10}(c/H_0/\text{Mpc}) + 25$ obtained from low- z SNe data ($0.01 \leq z \leq 0.2$) and the corresponding value obtained from the full Pantheon dataset. Here M is the color and stretch corrected absolute magnitude of SN Ia. Other work like [53] has also used the full data of Pantheon sample but the assumed model is the LTB model instead of the Λ LTB model. We therefore extend the analysis to the Λ LTB model by fitting the full Pantheon SNe data ranging from $0.01 < z < 2.3$ over all three parameters in the GBH parameterization for the matter density fraction. We confirm the previous findings that even in this general setting the local void cannot fully resolve the Hubble tension. The rest of this paper is organized as follows: In Sec. II, we introduce the Λ LTB model with GBH profile function. In Sec. III, we use the Pantheon data to constrain the GBH void profile. Section IV is devoted to conclusion and discussions.

II. GBH VOID IN Λ LTB MODEL

A. FLRW equation

As a generalization of the usual Friedman-Lemaître-Robertson-Walker (FLRW) metric within the framework of general relativity, the LTB metric [25–27] (see also [48]) uses the generalized scale factor $R(r, t)$ and a curvature

term $k(r)$ to describe an inhomogeneous but isotropic void by

$$ds^2 = dt^2 - \frac{R'^2(r, t)}{1 - k(r)} dr^2 - R^2(r, t) d\Omega^2, \quad (1)$$

with $R'(r, t) = \partial R(r, t)/\partial r$. Imposing the homogeneous condition $R(r, t) = a(t)r$ and $k(r) = kr^2$ would reduce the LTB metric into the FLRW metric with $a(t)$ acting as the usual cosmic scale factor and thus preserve the homogeneity and Copernican principle of our Universe. The corresponding Friedmann equation for the Λ LTB model reads

$$H^2(r, t) = H_0^2(r) \left[\Omega_M(r) \left(\frac{R_0(r)}{R(r, t)} \right)^3 + \Omega_k(r) \left(\frac{R_0(r)}{R(r, t)} \right)^2 + \Omega_\Lambda(r) \right], \quad (2)$$

where

$$H^2(r, t) \equiv \left(\frac{\dot{R}(r, t)}{R(r, t)} \right)^2 \quad (3)$$

is the Hubble parameter and the dot is taken for the derivative with respect to t . Hence $H_0(r) \equiv H(r, t_0)$ and $R_0(r) \equiv R(r, t_0)$. The Friedmann equation for the Λ LTB model at present time could also be written as $\Omega_M(r) + \Omega_k(r) + \Omega_\Lambda(r) = 1$.

B. GBH profile

If the matter density parameter outside the void $\Omega_{M,\text{out}}$ is assumed to be set by the CMB data, and the matter density parameter in the void interior $\Omega_M(r)$ exhibits explicit radial dependence, the fractional deficit could therefore be defined as

$$\delta(r) \equiv \frac{\Omega_M(r) - \Omega_{M,\text{out}}}{\Omega_{M,\text{out}}}, \quad (4)$$

which could be further parameterized by the dubbed GBH profile function [21,47,48] as

$$\delta(r) = \delta_V \frac{1 - \tanh((r - r_V)/2\Delta_r)}{1 + \tanh(r_V/2\Delta_r)}, \quad (5)$$

with δ_V , r_V , and Δ_r characterizing the depth, radius, and transition width of the void, respectively. An illustration for the GBH profile is shown in Fig. 1. Besides the GBH profile function describing a Universe with *two* “homogeneous” parts linked by a smooth function, there are many other profiles like those proposed in [54–56]. Therefore, the critical densities of matter, dark energy, and curvature could be obtained by

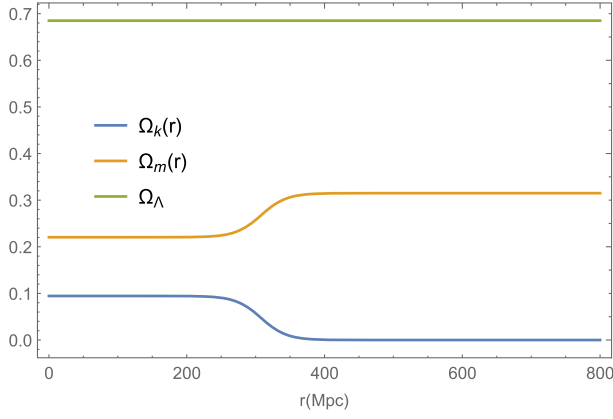


FIG. 1. The GBH profile with KBC void parameters $\delta_V = -0.3$, $r_V = 308$ Mpc and $\Delta_r = 18.46$ Mpc.

$$\Omega_M(r) = \Omega_{M,\text{out}}(1 + \delta(r)), \quad (6)$$

$$\Omega_\Lambda(r) = 1 - \Omega_{M,\text{out}}, \quad (7)$$

$$\Omega_k(r) = 1 - \Omega_M(r) - \Omega_\Lambda(r), \quad (8)$$

respectively, where $\Omega_\Lambda(r)$ is assumed to be a constant since it is not a diluted background parameter.

C. Synchronous comoving gauge

We choose the synchronous comoving gauge $R_0(r) = r$ for (2):

$$\begin{aligned} H^2(r, t) = & \Omega_{M,\text{out}}(1 + \delta(r))H_0^2(r) \left(\frac{r}{R(r, t)} \right)^3 \\ & - \Omega_{M,\text{out}}\delta(r)H_0^2(r) \left(\frac{r}{R(r, t)} \right)^2 \\ & + (1 - \Omega_{M,\text{out}})H_0^2(r), \end{aligned} \quad (9)$$

which, after integrated, gives rise to the age of the Universe of form

$$\begin{aligned} t_B(r) = & \int_0^r dR R^{-1} \left[\Omega_M(r)H_0^2(r) \left(\frac{r}{R} \right)^3 \right. \\ & \left. + \Omega_k(r)H_0^2(r) \left(\frac{r}{R} \right)^2 + \Omega_\Lambda(r)H_0^2(r) \right]^{-1/2}. \end{aligned} \quad (10)$$

For r at CMB scales with $\delta(r) = 0$, every physical parameter is in accordance with its CMB counterpart so that we can dismiss the difference between $t_B(r)$ and the real cosmic time $t_0(r)$ and set the universal cosmic time assumption $t_B(r) = t_B \equiv \text{const}$ [48], where t_B is the time at CMB scales:

$$t_B = \int_0^1 \frac{da_{\text{out}}(t)}{H_{0,\text{out}}[\Omega_{M,\text{out}}a_{\text{out}}^{-1} + \Omega_{\Lambda,\text{out}}a_{\text{out}}^2]^{1/2}}, \quad (11)$$

with $a_{\text{out}}(t)$ playing the role of the scale factor outside the void at CMB scales in accordance with its counterpart in FLRW metric. Now we can combine (10) and (11) to infer $H_0(r)$ as a function of the radial coordinate r . Furthermore, using the equations for null geodesics in the ALTB model could lead to the redshift z as a function of the radial coordinate r and the cosmic time t [48]:

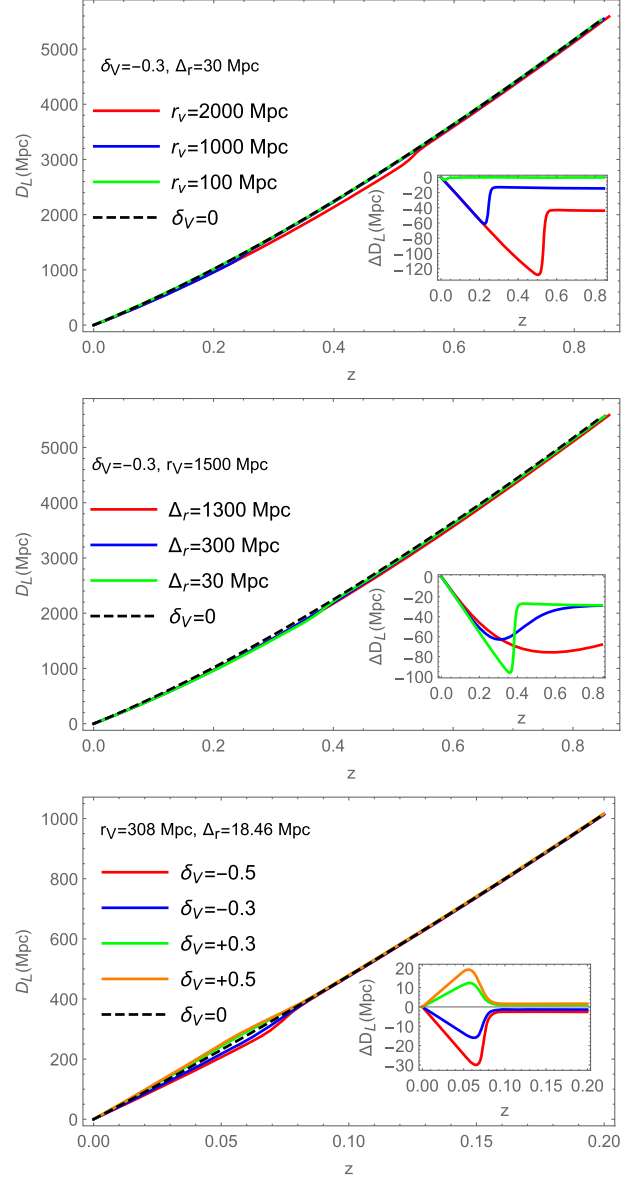


FIG. 2. The luminosity distance with respect to the redshift from the Λ CDM model (black dashed curve) and Λ LTB model (solid curves) with varying r_V (first panel), varying Δ_r (second panel), and varying δ_V (third panel), respectively, but with the other two parameters fixed as indicated in each panel. The subfigures present the differences of the corresponding Λ LTB models with respect to the Λ CDM model.

$$\begin{aligned} \frac{dt}{dr} &= -\frac{R'(r, t)}{\sqrt{1-k(r)}}, \\ \frac{1}{1+z} \frac{dz}{dr} &= \frac{\dot{R}'(r, t)}{\sqrt{1-k(r)}}, \end{aligned} \quad (12)$$

which could be inverted to rewrite the cosmic time t , the radial coordinate r and every other parameter within the void in terms of the redshift z including, for example, the luminosity distance:

$$d_L = (1+z)^2 R(r(z), t(z)). \quad (13)$$

To manifest the difference of using the Λ LTB model with respect to the Λ CDM model, the luminosity distance from varying one of the GBH parameters but fixing the other two GBH parameters has been presented in Fig. 2 with solid curves compared to the Λ CDM result shown as a black dashed curve.

III. DATA ANALYSIS AND COSMOLOGICAL CONSTRAINT

A. Data analysis

The data we use for analysis in this paper consist of 1048 SNe Ia ranging from $0.01 < z < 2.3$, which is summarized in the Pantheon sample [57] combining the following datasets with consistent photometry:

- (i) *Low- z data.*— $0.01 < z < 0.1$ from CfA1-4 [58–62] and CSP [63–65];
- (ii) *Intermediate- z data.*— $0.03 \lesssim z \lesssim 0.68$ from PS1 [66,67], $0.1 \lesssim z \lesssim 0.4$ from SDSS [68–70], and $0.3 \lesssim z \lesssim 1.1$ from SNLS [71,72];
- (iii) *High- z data.*— $z > 1.0$ from SCP [73], GOODS [74,75] and CANDELS/CLASH [76–78].

The above data will be tested for our Λ LTB model with GBH void profile function in the redshift-distance

relation (13), where the luminosity distance is measured as usual by the distance modulus:

$$\mu = m_B^0 - M_B^0 = 5 \log_{10} \left(\frac{d_L(z)}{\text{Mpc}} \right) + 25, \quad (14)$$

where m_B^0 is the corrected peak magnitude of a SN and M_B^0 is the absolute magnitude of a fiducial counterpart. It is worth noting that, for Pantheon data, it is necessary to consider the heliocentric redshift z_{Hel} in

$$\begin{aligned} \mu &= m_B^0 - M_B^0 \\ &= 5 \log_{10} \left(\frac{d_L(z_{\text{CMB}})}{\text{Mpc}} \right) + 5 \log_{10} \left(\frac{1+z_{\text{Hel}}}{1+z_{\text{CMB}}} \right) + 25. \end{aligned} \quad (15)$$

The test we adopt for data analysis is the usual χ^2 test [57]:

$$\chi^2 = \Delta \boldsymbol{\mu}^T \cdot \mathbf{C}^{-1} \cdot \Delta \boldsymbol{\mu}, \quad (16)$$

where $\Delta \boldsymbol{\mu} = \boldsymbol{\mu} - \boldsymbol{\mu}_{\Lambda\text{LTB}}$ and \mathbf{C} is the covariance matrix consisting of

$$\mathbf{C} = \mathbf{D}_{\text{stat}} + \mathbf{C}_{\text{sys}}. \quad (17)$$

\mathbf{D}_{stat} has only diagonal components containing the total distance errors associated with each SN, which include photometric error, mass step correction, distance bias correction, peculiar velocity uncertainty, redshift measurement uncertainty in quadrature, stochastic gravitational lensing and intrinsic scatter. \mathbf{C}_{sys} is the systematic covariance. The method we use for data analysis is the usual Markov chain Monte Carlo (MCMC) sampling [79] to scan all three parameters (r_V , Δ_r and δ_V) of the GBH profile in the Λ LTB model with respect to the Pantheon data [57] and the Λ CDM model calibrated by the Planck 2018 results $\Omega_{M,\text{out}} = 0.315 \pm 0.007$ and $H_{0,\text{out}} = (67.4 \pm 0.5) \text{ km/s/Mpc}$ [8]

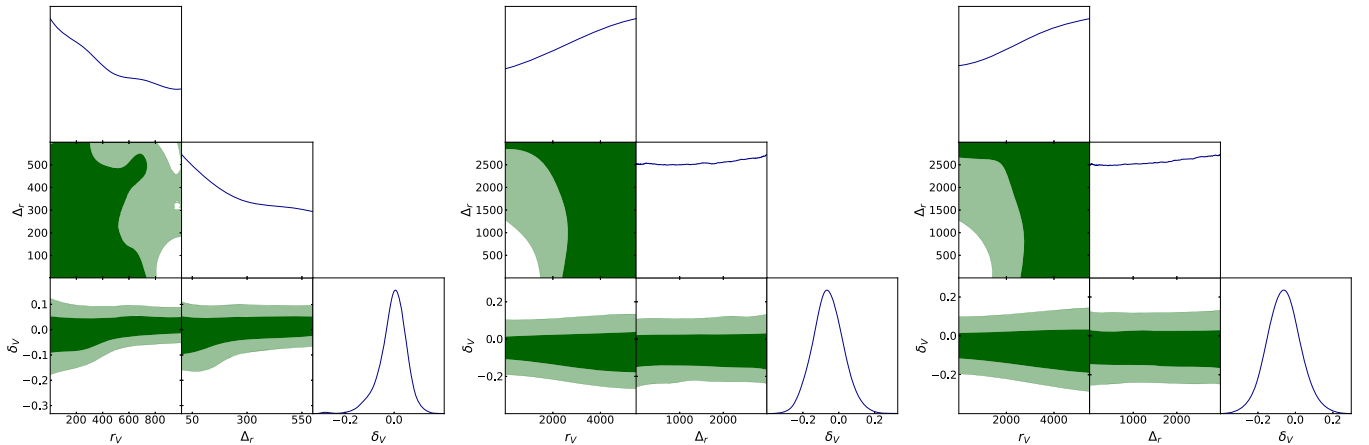


FIG. 3. Posterior constraints on δ_V , Δ_r and r_V from searching the void within redshift $z \leq 0.2$, $z \leq 1$, and $z \leq 2$, respectively. The contours describe the 68% and 95% confidence limits.

TABLE I. The cosmological constraints from the global fitting for the total Pantheon sample cut at different redshift ranges (first column) with corresponding number of SNe (second column) on the best-fit value (third column), mean value (fourth column), and standard deviation (fifth column) of the void depth δ_V , the best-fit value of the void radius r_V (sixth column), the best-fit value of the void transition width Δ_r (seventh column), the reduced χ^2 for the best-fit Λ LTB model (eighth column), the reduced χ^2 for the Λ CDM model (ninth column), the comparison to the Λ CDM model using the relative AIC values (tenth column), and the comparison to the Λ CDM model using the relative BIC values (11th column).

SNe range	SNe number	δ_V			r_V [Mpc]	Δ_r [Mpc]	$\chi^2_{\text{ALT B}} / \text{d.o.f.}$	$\chi^2_{\text{CDM}} / \text{d.o.f.}$	ΔAIC	ΔBIC
		Best fit	Mean	Std-dev						
$z \leq 0.2$	411	-9.1%	-5.6%	5.8%	334	1.71	0.988	0.988	2.61	17.47
$z \leq 1.0$	1025	-5.5%	-5.9%	8.7%	224	31.03	0.989	0.988	4.21	19.07
$z \leq 2.0$	1047	-6.2%	-6.2%	9.1%	1204	2.02	0.987	0.988	1.90	16.77

outside the void in order to match the CMB observations at large scales. Since we have no *a priori* setup for the void we want to identify by the Pantheon data alone; we therefore choose the following flat prior for all three parameters in the GBH parameterization with three illustrative redshift bins:

- (i) $z < 0.2$.— $r_V \in [1, 1000]$ Mpc, $\Delta_r \in [1, 600]$ Mpc, $\delta_V \in [-0.5, 0.5]$;
- (ii) $z < 1$.— $r_V \in [1, 5500]$ Mpc, $\Delta_r \in [1, 3000]$ Mpc, $\delta_V \in [-0.4, 0.4]$;
- (iii) $z < 2$.— $r_V \in [1, 5500]$ Mpc, $\Delta_r \in [1, 3000]$ Mpc, $\delta_V \in [-0.4, 0.4]$.

Note that the shortest distance to a supernova in our data sample is ~ 45 Mpc (CMB frame) and the local void search is limited within redshift $z \leq 2$ since most of SNe data of Pantheon sample are within redshift $z \leq 2$ (1047 of 1048 in total) so that the Λ LTB metric is reduced to the FLRW metric outside $z > 2$ with the homogeneous condition and $k(r) = kr^2$ automatically preserved.

B. Cosmological constraints

The cosmological constraints are shown in Fig. 3 and summarized in Table I, which are marginally consistent with the case of no local void $\delta_V = 0$ and there is seemingly no constraint on r_V and Δ_r simply because there is no difference between the inside and outside of the void in the case of $\delta_V = 0$. This is not surprising since r_V and Δ_r can only be strongly constrained when there is a strong preference for a large δ_V . On the other hand, if we want to search for any local void in the full data of Pantheon sample, then we have to allow for a nonzero δ_V , and there is no reason to fix r_V and Δ_r anymore, nor do we have any prior value for fixing r_V and Δ_r ; hence, we fit all three GBH parameters in this paper. Since at the limit of $\delta_V \rightarrow 0$ the void model reduces to the Λ CDM model and R/r is a function of t alone, namely the scale factor in Λ CDM model, the kSZ effect [33,34], the Rees-Sciama effect [80–82] and baryon acoustic oscillations would be in accordance with the Λ CDM model.

Therefore, our cosmological constraints are consistent with the Λ CDM model instead of the Λ LTB model with large δ_V in GBH parameterization for the void profile

within $z \leq 2$. At the very least, the Λ CDM model cannot be distinguished from the Λ LTB model with small δ_V constrained by the SNe data alone as shown in Fig. 4. Even if we could live in a void, the radial profile change is too insignificant to modify the concordance model.

Besides the χ^2 test, we also provide with the Akaike information criterion (AIC) [83] and Bayesian information criterion (BIC) tests [84], which are defined by $\text{AIC} = 2k - 2 \ln \hat{L}$ and $\text{BIC} = k \ln n - 2 \ln \hat{L}$, respectively, where k is the number of parameters for a given model, n is the number of data points, and \hat{L} is the maximized value of the likelihood function. A smaller AIC or BIC value means a better fitting for the given model. For model selection [85], we use the relative AIC or BIC value of the Λ LTB model with respect to the Λ CDM model. Therefore, a larger relative AIC or BIC value means that the Λ LTB model is less preferred compared to the Λ CDM model, and a more negative relative AIC or BIC value means that the v model is more favorable. As seen from the last two columns of Table I, there is no strong preference between the Λ LTB and Λ CDM models according to the relative AIC values ΔAIC . However, all the relative BIC values ΔBIC are

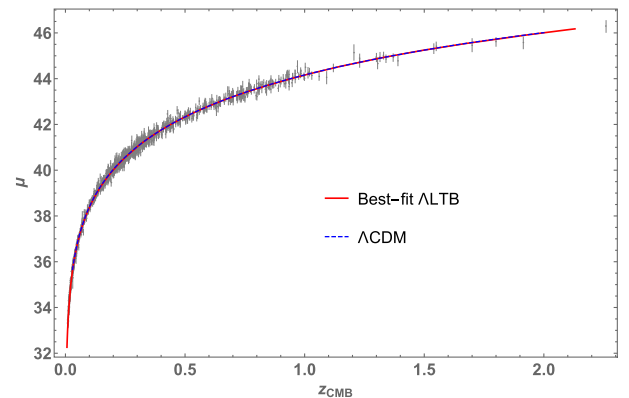


FIG. 4. Comparison of the distance modulus between the Λ LTB model (red solid line) with the best-fitting values constrained from SNe data within $z \leq 2$ and the Λ CDM model (blue dashed line) with values from Planck 2018 constraints. The Pantheon data are shown in gray.

TABLE II. The cosmological constraints from fitting over δ_V alone with the other two GBH parameters fixed at the KBC void parameters ($r_V = 308$ Mpc and $\Delta_r = 18.46$ Mpc) for the total Pantheon sample cut at different redshift ranges (first column) with corresponding number of SNe (second column) on the best-fit value (third column), mean value (fourth column), and standard deviation (fifth column) of the void depth δ_V , the reduced χ^2 for the best-fit Λ LTB model (sixth column), the reduced χ^2 for the Λ CDM model (seventh column), the comparison to Λ CDM model using the relative AIC values (eighth column), and the comparison to Λ CDM model using the relative BIC values (ninth column).

SNe range	SNe number	δ_V			$\chi^2_{\text{ALT}}/\text{d.o.f.}$	$\chi^2_{\text{CDM}}/\text{d.o.f.}$	ΔAIC	ΔBIC
		Best fit	Mean	Std-dev				
$z \leq 0.2$	411	-7.4%	-7.1%	4.8%	0.987	0.988	-0.40	4.55
$z \leq 1.0$	1025	-8.4%	-8.2%	4.5%	0.986	0.988	-1.09	3.87
$z \leq 2.0$	1047	-8.5%	-8.2%	4.7%	0.986	0.988	-1.12	3.84

larger than 10, which strongly disfavor the Λ LTB model over the Λ CDM model. To see how much improvement we can make from fitting all GBH parameters compared to a single parameter (δ_V) fitting, we have also fitted the Pantheon SNe data of different redshift ranges to the depth of cosmic void δ_V alone while fixing the other two GBH parameters at the KBC void parameters ($r_V = 308$ Mpc and $\Delta_r = 18.46$ Mpc). The relative AIC and BIC values of the Λ LTB model with respect to the Λ CDM model are summarized in the last two columns of Table II, which admit no preference for the Λ LTB model over Λ CDM model. Therefore, global fitting of all GBH parameters could lead to more dramatic disfavor of the Λ LTB model over the Λ CDM model.

To see how large δ_V is needed for resolving the Hubble tension, we depict the Hubble constant in local void $H_{0,\text{in}}$ as a function of δ_V assuming the Hubble constant at the CMB scales as $H_{0,\text{out}}$. It is easy to see that δ_V should be less than -30% to moderately resolve the Hubble tension as shown in Fig. 5, which is beyond the uncertainty region of δ_V even if all three GBH parameters are used in the data fitting.

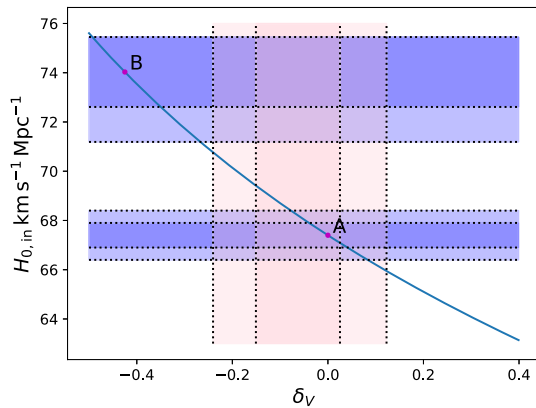


FIG. 5. The required δ_V for given H_0 inside a void described by our Λ LTB model, where “A” and “B” correspond to the Hubble constants from the Planck 2018 constraint and local measurement [13], respectively. The shaded regions are for 2σ uncertainty regions.

IV. CONCLUSION AND DISCUSSIONS

In this paper, we have constrained the Λ LTB model with GBH parameterization for the local void profile from the MCMC sampling in fitting the Pantheon data within $z \leq 2$. Our fitting results are consistent with the Λ CDM model and have no significant preference for a large local void to fully resolve the Hubble tension. However, the current analysis still merits further improvements to settle down the void issue when addressing the Hubble tension.

First, we have made a compromised choice for our GBH parameterization on the dimensionless matter density fraction instead of the physical matter density profile, the latter of which is quite challenging to implement in the numerical global fitting. The previous studies [48,51] evade this difficulty by either fixing the GBH parameters as the KBC void parameters [48] or parameterizing the spatial curvature in terms of the GBH profile with top-hat shape [51]. A GBH parameterization for the physical matter density profile in the global fitting would lead to the most general conclusion reserved for future study.

Second, we have not explored the global fitting constraint for the luminosity distance data from the galaxy survey that usually leads to the discovery of a large local void. It is unclear whether there is some unidentified systematic in the SNe data or galaxy survey data to reconcile their apparent disagreement when fitting to a local void.

ACKNOWLEDGMENTS

We thank Wei-Ming Dai, Chang Liu, De-Yu Wang, Wen-Hong Ruan, Jing Liu and Yong Zhou for the delightful discussions and help with code. This work is supported in part by the National Natural Science Foundation of China Grants No. 11690021, No. 11690022, No. 11851302, No. 11821505, and No. 11947302, in part by the Strategic Priority Research Program of the Chinese Academy of Sciences Grant No. XDB23030100 and No. XDA15020701; the Key Research Program of the CAS Grant No. XDPB15; and by Key Research Program of Frontier Sciences, CAS.

- [1] A. G. Riess *et al.* (Supernova Search Team Collaboration), Observational evidence from supernovae for an accelerating universe and a cosmological constant, *Astron. J.* **116**, 1009 (1998).
- [2] S. Perlmutter *et al.* (Supernova Cosmology Project Collaboration), Measurements of ω and λ from 42 high redshift supernovae, *Astrophys. J.* **517**, 565 (1999).
- [3] G. F. Smoot *et al.* (COBE Collaboration), Structure in the COBE differential microwave radiometer first year maps, *Astrophys. J. Lett.* **396**, L1 (1992).
- [4] D. N. Spergel *et al.* (WMAP Collaboration), First year Wilkinson Microwave Anisotropy Probe (WMAP) observations: Determination of cosmological parameters, *Astrophys. J. Suppl.* **148**, 175 (2003).
- [5] P. A. R. Ade *et al.* (Planck Collaboration), Planck 2013 results. I. Overview of products and scientific results, *Astron. Astrophys.* **571**, A1 (2014).
- [6] P. A. R. Ade *et al.* (Planck Collaboration), Planck 2013 results. XVI. Cosmological parameters, *Astron. Astrophys.* **571**, A16 (2014).
- [7] P. A. R. Ade *et al.* (Planck Collaboration), Planck 2015 results. XIII. Cosmological parameters, *Astron. Astrophys.* **594**, A13 (2016).
- [8] N. Aghanim *et al.* (Planck Collaboration), Planck 2018 results. VI. Cosmological parameters, *Astron. Astrophys.* **641**, A6 (2020).
- [9] A. G. Riess, L. Macri, S. Casertano, H. Lampeitl, H. C. Ferguson, A. V. Filippenko, S. W. Jha, W. Li, and R. Chornock, A 3% solution: Determination of the Hubble constant with the Hubble space telescope and wide field camera 3, *Astrophys. J.* **730**, 119 (2011); Erratum, *Astrophys. J.* **732**, 129 (2011).
- [10] A. G. Riess *et al.*, A 2.4% determination of the local value of the Hubble constant, *Astrophys. J.* **826**, 56 (2016).
- [11] A. G. Riess *et al.*, New parallaxes of galactic cepheids from spatially scanning the Hubble space telescope: Implications for the Hubble constant, *Astrophys. J.* **855**, 136 (2018).
- [12] A. G. Riess *et al.*, Milky Way cepheid standards for measuring cosmic distances and application to Gaia DR2: Implications for the Hubble constant, *Astrophys. J.* **861**, 126 (2018).
- [13] A. G. Riess, S. Casertano, W. Yuan, L. M. Macri, and D. Scolnic, Large magellanic cloud cepheid standards provide a 1% foundation for the determination of the Hubble constant and stronger evidence for physics beyond Λ CDM, *Astrophys. J.* **876**, 85 (2019).
- [14] D. Camarena and V. Marra, Local determination of the Hubble constant and the deceleration parameter, *Phys. Rev. Research* **2**, 013028 (2020).
- [15] K. C. Wong *et al.*, H0LiCOW—XIII. A 2.4 per cent measurement of H_0 from lensed quasars: 5.3σ tension between early- and late-Universe probes, *Mon. Not. R. Astron. Soc.* **498**, 1420 (2020).
- [16] L. Verde, T. Treu, and A. G. Riess, Tensions between the early and the late Universe, *Nat. Astron.* **3**, 891 (2019).
- [17] W. L. Freedman, Cosmology at a crossroads, *Nat. Astron.* **1**, 0121 (2017).
- [18] Y. Park and E. Rozo, Concordance cosmology? *Mon. Not. R. Astron. Soc.* **499**, 4638 (2020).
- [19] L. Knox and M. Millea, Hubble constant hunter's guide, *Phys. Rev. D* **101**, 043533 (2020).
- [20] R. C. Keenan, A. J. Barger, L. L. Cowie, W. H. Wang, I. Wold, and L. Trouille, Testing for a large local void by investigating the near-infrared galaxy luminosity function, *Astrophys. J.* **754**, 131 (2012).
- [21] R. C. Keenan, A. J. Barger, and L. L. Cowie, Evidence for a 300 megaparsec scale under-density in the local galaxy distribution, *Astrophys. J.* **775**, 62 (2013).
- [22] J. R. Whitbourn and T. Shanks, The local hole revealed by galaxy counts and redshifts, *Mon. Not. R. Astron. Soc.* **437**, 2146 (2014).
- [23] J. R. Whitbourn and T. Shanks (Extragalactic Astronomy Group and Durham University Collaboration), The galaxy luminosity function and the Local Hole, *Mon. Not. R. Astron. Soc.* **459**, 496 (2016).
- [24] H. Böhringer, G. Chon, and C. A. Collins, Observational evidence for a local underdensity in the Universe and its effect on the measurement of the Hubble constant, *Astron. Astrophys.* **633**, A19 (2020).
- [25] G. Lemaitre, The expanding universe, *Gen. Relativ. Gravit.* **29**, 641 (1997).
- [26] R. C. Tolman, Effect of inhomogeneity on cosmological models, *Proc. Natl. Acad. Sci. U.S.A.* **20**, 169 (1934).
- [27] H. Bondi, Spherically symmetrical models in general relativity, *Mon. Not. R. Astron. Soc.* **107**, 410 (1947).
- [28] M.-N. Celerier, Do we really see a cosmological constant in the supernovae data? *Astron. Astrophys.* **353**, 63 (2000), <https://ui.adsabs.harvard.edu/abs/2000A%26A...353...63C/abstract>.
- [29] C.-M. Yoo, K.-i. Nakao, and M. Sasaki, CMB observations in LTB universes: Part I: Matching peak positions in the CMB spectrum, *J. Cosmol. Astropart. Phys.* **07** (2010) 012.
- [30] V. Marra, E. W. Kolb, S. Matarrese, and A. Riotto, On cosmological observables in a Swiss-Cheese universe, *Phys. Rev. D* **76**, 123004 (2007).
- [31] N. Brouzakis, N. Tzavara, and E. Tzavara, Light propagation and large-scale inhomogeneities, *J. Cosmol. Astropart. Phys.* **04** (2008) 008.
- [32] K. Kainulainen and V. Marra, SNe observations in a meatball universe with a local void, *Phys. Rev. D* **80**, 127301 (2009).
- [33] R. Sunyaev and Y. Zeldovich, The observations of relic radiation as a test of the nature of x-ray radiation from the clusters of galaxies, *Comments Astrophys. Space Phys.* **4**, 173 (1972), <https://inspirehep.net/literature/76585>.
- [34] R. Sunyaev and Y. Zeldovich, The velocity of clusters of galaxies relative to the microwave background. The possibility of its measurement, *Mon. Not. R. Astron. Soc.* **190**, 413 (1980).
- [35] P. Zhang and A. Stebbins, Confirmation of the Copernican Principle at Gpc Radial Scale and Above from the Kinetic Sunyaev Zel'dovich Effect Power Spectrum, *Phys. Rev. Lett.* **107**, 041301 (2011).
- [36] Q. Ding, T. Nakama, and Y. Wang, A gigaparsec-scale local void and the Hubble tension, *Sci. China Phys. Mech. Astron.* **63**, 290403 (2020).
- [37] V. Marra, L. Amendola, I. Sawicki, and W. Valkenburg, Cosmic Variance and the Measurement of the Local Hubble Parameter, *Phys. Rev. Lett.* **110**, 241305 (2013).

- [38] H.-Y. Wu and D. Huterer, Sample variance in the local measurements of the Hubble constant, *Mon. Not. R. Astron. Soc.* **471**, 4946 (2017).
- [39] D. Camarena and V. Marra, Impact of the cosmic variance on H_0 on cosmological analyses, *Phys. Rev. D* **98**, 023537 (2018).
- [40] M. Tokutake, K. Ichiki, and C.-M. Yoo, Observational constraint on spherical inhomogeneity with CMB and local Hubble parameter, *J. Cosmol. Astropart. Phys.* **03** (2018) 033.
- [41] B. L. Hoscheit and A. J. Barger, The KBC void: Consistency with supernovae type Ia and the kinematic SZ effect in a ALTB model, *Astrophys. J.* **854**, 46 (2018).
- [42] T. Shanks, L. Hogarth, and N. Metcalfe, Gaia cepheid parallaxes and 'local hole' relieve H_0 tension, *Mon. Not. R. Astron. Soc.* **484**, L64 (2019).
- [43] A. Lawrence *et al.*, The UKIRT infrared deep sky survey (UKIDSS), *Mon. Not. R. Astron. Soc.* **379**, 1599 (2007).
- [44] S. P. Driver and A. S. G. Robotham, Quantifying cosmic variance, *Mon. Not. R. Astron. Soc.* **407**, 2131 (2010).
- [45] S. P. Driver *et al.*, Galaxy and mass assembly (GAMA): Survey diagnostics and core data release, *Mon. Not. R. Astron. Soc.* **413**, 971 (2011).
- [46] G. Lavaux and M. J. Hudson, The 2M++ galaxy redshift catalogue, *Mon. Not. R. Astron. Soc.* **416**, 2840 (2011).
- [47] J. Garcia-Bellido and T. Haugboelle, Confronting Lemaitre-Tolman-Bondi models with observational cosmology, *J. Cosmol. Astropart. Phys.* **04** (2008) 003.
- [48] W. D. Kenworthy, D. Scolnic, and A. Riess, The local perspective on the Hubble tension: Local structure does not impact measurement of the Hubble constant, *Astrophys. J.* **875**, 145 (2019).
- [49] R. Wojtak, A. Knebe, W. A. Watson, I. T. Iliev, S. Heß, D. Rapetti, G. Yepes, and S. Gottlöber, Cosmic variance of the local Hubble flow in large-scale cosmological simulations, *Mon. Not. R. Astron. Soc.* **438**, 1805 (2014).
- [50] I. Odderskov, S. Hannestad, and T. Haugbølle, On the local variation of the Hubble constant, *J. Cosmol. Astropart. Phys.* **10** (2014) 028.
- [51] V. V. Luković, B. S. Haridasu, and N. Vittorio, Exploring the evidence for a large local void with supernovae Ia data, *Mon. Not. R. Astron. Soc.* **491**, 2075 (2020).
- [52] L. Kazantzidis and L. Perivolaropoulos, Hints of a local matter underdensity or modified gravity in the low z Pantheon data, *Phys. Rev. D* **102**, 023520 (2020).
- [53] D. Sapone, S. Nesseris, and C. A. P. Bengaly, Is there any measurable redshift dependence on the SN Ia absolute magnitude? *Phys. Dark Universe* **32**, 100814 (2021).
- [54] C. Z. Vargas, F. T. Falciano, and R. R. R. Reis, Constraining LTb models with JLA supernovae and BAO, [arXiv:1512.02571](https://arxiv.org/abs/1512.02571).
- [55] S. February, J. Larena, M. Smith, and C. Clarkson, Rendering dark energy void, *Mon. Not. R. Astron. Soc.* **405**, 2231 (2010).
- [56] K. Enqvist and T. Mattsson, The effect of inhomogeneous expansion on the supernova observations, *J. Cosmol. Astropart. Phys.* **02** (2007) 019.
- [57] D. M. Scolnic *et al.*, The complete light-curve sample of spectroscopically confirmed SNe Ia from Pan-STARRS1 and cosmological constraints from the combined pantheon sample, *Astrophys. J.* **859**, 101 (2018).
- [58] A. G. Riess *et al.*, BV RI light curves for 22 type Ia supernovae, *Astron. J.* **117**, 707 (1999).
- [59] S. Jha *et al.*, Ubvri light curves of 44 type Ia supernovae, *Astron. J.* **131**, 527 (2006).
- [60] M. Hicken, P. Challis, S. Jha, R. P. Kirshner, T. Matheson, M. Modjaz, A. Rest, and W. M. Wood-Vasey, CfA3: 185 type Ia supernova light curves from the CfA, *Astrophys. J.* **700**, 331 (2009).
- [61] M. Hicken, W. M. Wood-Vasey, S. Blondin, P. Challis, S. Jha, P. L. Kelly, A. Rest, and R. P. Kirshner, Improved dark energy constraints from 100 new CfA supernova type Ia light curves, *Astrophys. J.* **700**, 1097 (2009).
- [62] M. Hicken *et al.*, CfA4: Light curves for 94 type Ia supernovae, *Astrophys. J. Suppl.* **200**, 12 (2012).
- [63] C. Contreras *et al.*, The Carnegie Supernova Project: First photometry data release of low-redshift type Ia supernovae, *Astron. J.* **139**, 519 (2010).
- [64] G. Folatelli *et al.*, The Carnegie Supernova Project: Analysis of the first sample of low-redshift type-Ia supernovae, *Astron. J.* **139**, 120 (2010).
- [65] M. D. Stritzinger *et al.*, The Carnegie Supernova Project: Second photometry data release of low-redshift type Ia Supernovae, *Astron. J.* **142**, 156 (2011).
- [66] A. Rest *et al.*, Cosmological constraints from measurements of type Ia supernovae discovered during the first 1.5 yr of the Pan-STARRS1 survey, *Astrophys. J.* **795**, 44 (2014).
- [67] D. Scolnic *et al.*, Systematic uncertainties associated with the cosmological analysis of the first Pan-STARRS1 type Ia supernova sample, *Astrophys. J.* **795**, 45 (2014).
- [68] J. A. Frieman *et al.*, The Sloan Digital Sky Survey-II supernova survey: Technical summary, *Astron. J.* **135**, 338 (2008).
- [69] R. Kessler *et al.*, First-year Sloan Digital Sky Survey-II (SDSS-II) supernova results: Hubble diagram and cosmological parameters, *Astrophys. J. Suppl.* **185**, 32 (2009).
- [70] M. Sako *et al.* (SDSS Collaboration), The data release of the Sloan Digital Sky Survey-II supernova survey, *Publ. Astron. Soc. Pac.* **130**, 064002 (2018).
- [71] A. Conley *et al.* (SNLS Collaboration), Supernova constraints and systematic uncertainties from the first 3 years of the supernova legacy survey, *Astrophys. J. Suppl.* **192**, 1 (2011).
- [72] M. Sullivan *et al.* (SNLS Collaboration), SNLS3: Constraints on dark energy combining the supernova legacy survey three year data with other probes, *Astrophys. J.* **737**, 102 (2011).
- [73] N. Suzuki *et al.* (Supernova Cosmology Project Collaboration), The Hubble space telescope cluster supernova survey: V. Improving the dark energy constraints above $z > 1$ and building an early-type-hosted supernova sample, *Astrophys. J.* **746**, 85 (2012).
- [74] A. G. Riess *et al.* (Supernova Search Team Collaboration), Type Ia supernova discoveries at $z > 1$ from the Hubble Space Telescope: Evidence for past deceleration and constraints on dark energy evolution, *Astrophys. J.* **607**, 665 (2004).
- [75] A. G. Riess *et al.*, New Hubble space telescope discoveries of Type Ia supernovae at $z \geq 1$: Narrowing constraints on

- the early behavior of dark energy, *Astrophys. J.* **659**, 98 (2007).
- [76] S. A. Rodney *et al.*, Type Ia supernova rate measurements to redshift 2.5 from CANDELS: Searching for prompt explosions in the early Universe, *Astron. J.* **148**, 13 (2014).
- [77] O. Graur *et al.*, Type-Ia supernova rates to redshift 2.4 from CLASH: The cluster lensing and supernova survey with Hubble, *Astrophys. J.* **783**, 28 (2014).
- [78] A. G. Riess *et al.*, Type Ia supernova distances at redshift > 1.5 from the Hubble space telescope multi-cycle treasury programs: The early expansion rate, *Astrophys. J.* **853**, 126 (2018).
- [79] A. Lewis and S. Bridle, Cosmological parameters from CMB and other data: A Monte Carlo approach, *Phys. Rev. D* **66**, 103511 (2002).
- [80] M. J. Rees and D. W. Sciama, Large scale density inhomogeneities in the universe, *Nature (London)* **217**, 511 (1968).
- [81] B. R. Granett, M. C. Neyrinck, and I. Szapudi, Dark energy detected with supervoids and superclusters, [arXiv:0805.2974](https://arxiv.org/abs/0805.2974).
- [82] I. Masina and A. Notari, The cold spot as a large void: Rees-Sciama effect on CMB power spectrum and bispectrum, *J. Cosmol. Astropart. Phys.* **02** (2009) 019.
- [83] H. Akaike, A new look at the statistical model identification, *IEEE Trans. Autom. Control* **19**, 716 (1974).
- [84] G. Schwarz, Estimating the dimension of a model, *Ann. Stat.* **6**, 461 (1978).
- [85] A. R. Liddle, Information criteria for astrophysical model selection, *Mon. Not. R. Astron. Soc.* **377**, L74 (2007).